

# Calculating anisotropic physical properties from texture data using the MTEX open source package

David Mainprice<sup>1</sup>, Ralf Hielscher<sup>2</sup>, Helmut Schaeben<sup>3</sup>

February 10, 2011

<sup>1</sup>*Geosciences Montpellier UMR CNRS 5243, Université Montpellier 2, 34095 Montpellier Cedex 05, France*

<sup>2</sup>*Fakultät für Mathematik, Technische Universität Chemnitz, 09126 Chemnitz, Germany*

<sup>3</sup>*Mathematische Geologie und Geoinformatik, Institut für Geophysik und Geoinformatik, Technische Universität Freiberg, 09596 Freiberg, Germany*

submitted to Deformation Mechanism, Rheology & Tectonics: Microstructures, Mechanics & Anisotropy - The Martin Casey Volume. In: Prior, D., Rutter, E.H., Tatham, D. J. (eds) Geological Society of London, Special Publication

REVISED VERSION 8/02/2011 DM

## Abstract

This paper presents the theoretical background for the calculation of physical properties of an aggregate from constituent crystal properties and the texture of the aggregate in a coherent manner. Emphasis is placed on the important tensor properties of 2<sup>nd</sup> and 4<sup>th</sup> rank with applications in rock deformation, structural geology, geodynamics and geophysics. We cover texture information that comes from pole figure diffraction and single orientation measurements (Electron Backscattered Diffraction, Electron Channeling Pattern, Laue Pattern, Optical microscope universal-stage). In particular, we give explicit formulas for the calculation of the averaged tensor from individual orientations or from an ODF. For the latter we consider numerical integration and an approach based on the expansion into spherical harmonics. This paper also serves as a reference paper for the tensor mathematic capabilities of the texture analysis software MTEX, which is a comprehensive, freely available MATLAB toolbox that covers a wide range of problems in quantitative texture analysis, e.g. orientation distribution function (ODF) modeling, pole figure to ODF inversion, EBSD data analysis, and grain detection. MTEX offers a programming interface, which allows the processing of involved research problems, as well as highly customizable visualization capabilities, which makes it perfect for scientific presentations, publications and teaching demonstrations.

**Keywords:** physical properties, tensors, texture, orientation density function, crystallographic preferred orientation, averaging methods, EBSD

# 1 Introduction

The estimation of physical properties of crystalline aggregates from the properties of the component crystals has been subject of extensive literature since the classical work of Voigt (1928) and Reuss (1929). Such an approach is only feasible if the bulk properties of the crystals dominate the physical property of the aggregate and the effects of grain boundary interfaces can be ignored. For example, the methods discussed here cannot be applied to the electrical properties of water-saturated rock, where the role of interfacial conduction is likely to be important. Many properties of interest to earth and materials scientists can be evaluated from the knowledge of the single crystal tensors and the orientation distribution function (ODF) of crystals in an aggregate, for example thermal diffusivity, thermal expansion, diamagnetism and elastic wave velocities.

The majority of rock-forming minerals have strongly anisotropic physical properties and many rocks also have strong crystal preferred orientations (CPOs, or textures as they are called in Materials Science) that can be described concisely in a quantitative manner by the *orientation density function* ODF. The combination of strong CPOs and anisotropic single crystal properties results in a three dimensional variation in rock properties. Petrophysical measurements are usually made under hydrostatic pressure, and often at high temperature to simulate conditions in the Earth, where presumably the micro-cracks present at ambient conditions are closed. The necessity to work at high pressure and temperature conditions limits the number of orientations that can be measured. Typically, three orthogonal directions are measured parallel to structural features, such as the lineation and foliation normal defined by grain shape. The evaluation of physical properties from CPO allows the determination of properties over the complete orientation sphere of the specimen reference frame.

This paper is designed as a reference paper for earth and material scientists who want to use the texture analysis software MTEX to compute physical tensor properties of aggregates from constituent crystal properties and the texture of the aggregate. MTEX is a comprehensive, freely available MATLAB toolbox that covers a wide range of problems in quantitative texture analysis, e.g. ODF modeling, pole figure to ODF inversion, EBSD data analysis, and grain detection. The MTEX toolbox can be downloaded from <http://mtex.googlecode.com>. Unlike many other texture analysis software, it offers a programming interface, which allows for the efficient processing of complex research problems in the form of scripts (M-files). The MATLAB environment provides a wide variety of high quality graphics file format to aid publication and display of the results. In addition the MTEX toolbox will work identically on Microsoft Windows, Apple Mac OSX and Linux platforms in 32 and 64 bit modes with a simple installation procedure.

In MTEX texture analysis information like ODFs, EBSD data, pole figures, are represented by variables of different types. For example, in order to define a unimodal ODF with half-width  $10^\circ$ , preferred orientation ( $10^\circ, 20^\circ, 30^\circ$ ) Euler angles and cubic crystal symmetry, one issues the command

```
myODF = unimodalODF(orientation('Euler',10*degree,20*degree,30*degree),...  
symmetry('cubic'),'halfwidth',10*degree)
```

64 which generates a variable `myodf` of type ODF which is displayed as

```
65 myODF = ODF
66   specimen symmetry: triclinic
67   crystal symmetry : cubic
68
69   Radially symmetric portion:
70     kernel: de la Vallee Poussin, hw = 10
71     center: (10,20,30)
72     weight: 1
```

73 We will keep this style of displaying input and output to make the syntax of MTEX as clear  
74 as possible. Note that there is also an exhaustive interactive documentation included in  
75 MTEX, which explains the syntax of each command in detail.

76 The outline of the paper is as follows. In the first section the basics of tensors mathemat-  
77 ics and crystal geometry are briefly mentioned and presented in terms of MTEX commands.  
78 In the second section these basics are discussed for some classical second order tensors and  
79 the elasticity tensors. In particular we give a comprehensive overview about elastic prop-  
80 erties that can be computed directly from the elastic stiffness tensor. All calculations are  
81 accompanied by the corresponding MTEX commands. In the third section we are concerned  
82 with the calculation of average matter tensors from their single crystal counterparts and  
83 the texture of the aggregate. Here we consider textures given by individual orientation  
84 measurements, which leads to the well known Voigt, Reuss, and Hill averages, as well as  
85 textures given by ODFs, which leads to formulas involving integrals over the orientation  
86 space. We can compute these integrals in several ways. Either we use known quadra-  
87 ture rule, or we compute the expansion of the rotated tensor into generalized spherical  
88 harmonics and apply Parseval's theorem. Explicit formulae for the expansion of a tensor  
89 into generalized spherical harmonics and a proof that the order of the tensor defines the  
90 maximum order of this expansion is included in the appendix.

## 91 2 Tensor mathematics and crystal geometry

92 In what follows we give the necessary background to undertake physical property calcula-  
93 tion for single crystals, without necessarily the full mathematical developments that can be  
94 found elsewhere (e.g. Nye, 1985). We will restrict ourselves to linear physical properties,  
95 that are properties than can be described by a linear relationship between cause and effect,  
96 such as stress and strain for linear elasticity.

### 97 2.1 Tensors

Mathematically, a tensor  $T$  of rank  $r$  is a  $r$ -linear mapping which can be represented by  
an  $r$ -dimensional matrix  $T_{i_1, i_2, \dots, i_r}$ . Thus a rank zero tensor is simply a scalar value, a rank  
one tensor  $T_i$  is a vector, and a rank two tensor  $T_{ij}$  has the form of a matrix. Linearity

means that the tensor applied to  $r$  vectors  $x^1, \dots, x^r \in \mathbb{R}^3$ , defines a mapping

$$(x^1, \dots, x^r) \mapsto \sum_{i_1=1}^3 \sum_{i_2=1}^3 \cdots \sum_{i_r=1}^3 T_{i_1, \dots, i_r} x_{i_1}^1 \cdots x_{i_r}^r$$

98 which is linear in each of the arguments  $x^1, \dots, x^r$ .

Physically, tensors are used to describe linear interactions between physical properties. In the simplest case, scalar properties are modelled by rank zero tensor, whereas vector fields, i.e., direction dependent properties, are modelled by rank one tensors. An example for a second rank tensor is the thermal conductivity tensor  $k_{ij}$  which describes the linear relationship between the negative temperature gradient  $-\text{grad}T = -(\frac{\partial T}{\partial x_1}, \frac{\partial T}{\partial x_2}, \frac{\partial T}{\partial x_3})$ , i.e. a first order tensor, and the heat flux  $q = (q_1, q_2, q_3)$  per unit area which is also an first order tensor. The linear relationship is given by the equality

$$q_i = - \sum_{j=1}^3 k_{ij} \frac{\partial T}{\partial x_j}, \quad i = 1, \dots, 3,$$

99 and can be seen as a matrix vector product of the thermal conductivity tensor  $k_{ij}$  inter-  
100 preted as a matrix and the negative temperature gradient interpreted as a vector. In the  
101 present example the negative temperature gradient is called *applied tensor* and the heat  
102 flux is called *induced tensor*.

In the general case, we define a rank  $r$  tensor  $T_{i_1, \dots, i_r}$ , inductively, as the linear relationship between two physical properties which are modelled by a rank  $s$  tensor  $A_{j_1, j_2, \dots, j_s}$  and a rank  $t$  tensor  $B_{k_1, k_2, \dots, k_t}$ , such that the equation  $r = t + s$  is satisfied. So the rank of a tensor is given by the rank of the induced tensor plus the rank of the applied tensor. The linear dependency between the applied tensor  $A$  and the induced tensor  $B$  is given by the tensor product

$$B_{k_1, \dots, k_t} = \sum_{j_1=1}^3 \sum_{j_2=1}^3 \cdots \sum_{j_s=1}^3 T_{k_1, k_2, \dots, k_t, j_1, \dots, j_s} A_{j_1, \dots, j_s} = T_{k_1, k_2, \dots, k_t, j_1, \dots, j_s} A_{j_1, \dots, j_s}$$

103 In the right hand side of the last equation we used the Einstein summation convention  
104 and omitted the sum sign for every two equal indexes. This will be default in all further  
105 formulae.

106 In MTEX a tensor is represented by a variable of type `tensor`. In order to create such a  
107 variable, the  $r$ -dimensional matrix has to be specified. As an example we consider the 2<sup>nd</sup>  
108 rank stress tensor  $\sigma_{ij}$ , which can be defined by

```
109 M = [[1.45 0.00 0.19]; ...
110       [0.00 2.11 0.00]; ...
111       [0.19 0.00 1.79]];
112
113 sigma = tensor(M, 'name', 'stress', 'unit', 'MPa');
```

```

114 sigma = stress tensor (size: 3 3)
115     rank: 2
116     unit: MPa
117
118     1.45  0.00  0.19
119     0.00  2.11  0.00
120     0.19  0.00  1.79

```

121 Furthermore, we defined the normal  $\vec{n} = (1, 0, 0)$  to plane by

```

122 n = vector3d(1,0,0)

```

```

123 n = vector3d (size: 1 1)
124   x  y  z
125   1  0  0

```

Then according to Cauchy's stress principle the stress vector  $T^{\vec{n}}$  associated with the plane normal  $\vec{n}$ , is computed by

$$T_j^{\vec{n}} = \sigma_{ij} \vec{n}_i.$$

126 In MTEX this equation may be written as

```

127 T = EinsteinSum(sigma, [-1 1], n, -1, 'unit', 'MPa')

```

```

128 T = tensor (size: 3)
129     unit: MPa
130     rank: 1
131
132     1.45
133     0
134     0.19

```

Note that the  $-1$  in the arguments of the command `EinsteinSum` indicates the dimension which has to be summed up and the  $1$  in the argument indicates that the second dimension of  $\sigma$  becomes the first dimension of  $T$ . Using the stress vector  $T^{\vec{n}}$  the scalar magnitudes of the normal stress  $\sigma_N$  and the shear stress  $\sigma_S$  are given as

$$\sigma_N = T_i^{\vec{n}} \vec{n}_i = \sigma_{ij} \vec{n}_i \vec{n}_j \text{ and } \sigma_S = \sqrt{T_i^{\vec{n}} T_i^{\vec{n}} - \sigma_N^2}.$$

135 In MTEX the corresponding calculation reads as

```

136 sigmaN = double(EinsteinSum(T, -1, n, -1))
137 sigmaS = sqrt(double(EinsteinSum(T, -1, T, -1)) - sigmaN^2)

```

```

138 sigmaN =
139
140     1.4500
141
142 sigmaS =
143
144     0.1900

```

crystal symmetries	$\vec{X}^T$	$\vec{Y}^T$	$\vec{Z}^T$
orthorhombic, tetragonal, cubic	$\vec{a}$	$\vec{b}$	$\vec{c}$
trigonal, hexagonal	$\vec{a}$	$\vec{m}$	$\vec{c}$
	$\vec{m}$	$-\vec{a}$	$\vec{c}$
monoclinic	$\vec{a}^*$	$\vec{b}$	$\vec{c}$
	$\vec{a}$	$\vec{b}$	$\vec{c}^*$
triclinic	$\vec{a}^*$	$\vec{Z}^T \times \vec{X}^T$	$\vec{c}$
	$\vec{a}$	$\vec{Z}^T \times \vec{X}^T$	$\vec{c}^*$
	$\vec{Y}^T \times \vec{Z}^T$	$\vec{b}^*$	$\vec{c}$
	$\vec{Y}^T \times \vec{Z}^T$	$\vec{b}$	$\vec{c}^*$

Table 1: Alignment of the crystal reference frame for the tensors of physical properties of crystals. The letters  $\vec{a}, \vec{b}, \vec{c}, \vec{m}$  correspond to crystallographic directions in the direct lattice space, whereas the letters  $\vec{a}^*, \vec{b}^*, \vec{c}^*$  denote the corresponding directions in the reciprocal lattice space, which are parallel to the normal to the plane written as  $\perp a$  for  $\vec{a}^*$  etc. N.B. there are atleast two possible reference choices for all symmetries except orthorhombic, tetragonal and cubic.

## 2.2 The crystal reference frame

Tensors can be classified into two types: matter tensors describing physical properties like electrical or thermal conductivity, magnetic permeability, etc., of a crystalline specimen, and field tensors describing applied forces, like stress, strain, or a electric field, to a specimen. Furthermore, it is important to distinguish between single crystal tensors describing constituent crystal properties and tensors describing averaged macroscopic properties of a polycrystalline specimen. While the reference frame for the latter ones is the specimen coordinate system, the reference frame for single crystal tensor properties is unambiguously connected with the crystal coordinate system. The reference frames and their conventions are explained below. We will restrict ourselves to tensors of single or polycrystals defined in a Cartesian reference frame comprising 3 unit vectors,  $\vec{X}^T, \vec{Y}^T, \vec{Z}^T$ . The use of an orthogonal reference frame for single crystals avoids the complications of the metric associated with the crystal unit cell axes. In any case, almost all modern measurements of physical property tensors are reported using Cartesian reference frames.

Next we discuss how the single crystal tensor reference frame is defined using the crystal coordinate system. In the general case of triclinic crystal symmetry, the crystal coordinate system is specified by its axis lengths  $a, b, c$  and inter-axial angles  $\alpha, \beta, \gamma$  resulting in a non Euclidean coordinate system  $\vec{a}, \vec{b}, \vec{c}$  for the general case. In order to align the Euclidean tensor reference frame  $\vec{X}^T, \vec{Y}^T, \vec{Z}^T$  in the crystal coordinate system several conventions are in use. The most common ones are summarized in Table 1.

In MTEX the alignment of the crystal reference frame is defined together with the symmetry group and the crystal coordinate system. All this information is stored in a variable

167 of type `symmetry`. For example by

```
168 cs_tensor = symmetry('triclinic',[5.29,9.18,9.42],...
169 [90.4,98.9,90.1]*degree, 'X||a*', 'Z||c', 'mineral', 'Talc');
```

```
170 cs_tensor = symmetry (size: 1)
171
172 mineral          : Talc
173 symmetry         : triclinic (-1)
174 a, b, c          : 5.3, 9.2, 9.4
175 alpha, beta, gamma: 90.4, 98.9, 90.1
176 reference frame  : X||a*, Z||c
```

177 we store in the variable `cs_tensor` the geometry of Talc which has triclinic crystal symme-  
 178 try, axes length 5.29, 9.18, 9.42, inter-axial angles  $90.4^\circ$ ,  $98.9^\circ$ ,  $90.1^\circ$ , and the convention for  
 179 a Cartesian right-handed tensor reference frame  $\vec{X}||\vec{a}^*$ ,  $\vec{Z}||\vec{c}$  and hence  $\vec{Y} = \vec{Z} \times \vec{X}$  for the  
 180 alignment of the crystal reference frame. In order to define a crystal constituent property  
 181 tensor with respect to this crystal reference frame we append the variable `cs_tensor` to  
 182 its definition, i.e.,

```
183 M = [[219.83  59.66  -4.82  -0.82  -33.87  -1.04];...
184      [ 59.66  216.38  -3.67  1.79  -16.51  -0.62];...
185      [-4.82  -3.67  48.89  4.12  -15.52  -3.59];...
186      [-0.82  1.79  4.12  26.54  -3.60  -6.41];...
187      [-33.87 -16.51 -15.52 -3.60  22.85  -1.67];...
188      [-1.04  -0.62  -3.59  -6.41  -1.67  78.29]];
189
190 C = tensor(M, 'name', 'elastic_stiffness', 'unit', 'GPa', cs_tensor)
```

```
191 C = elastic stiffness tensor (size: 3 3 3 3)
192   unit: GPa
193   rank: 4
194   mineral: Talc (triclinic, X||a*, Z||c)
195
196   tensor in Voigt matrix representation
197   219.83    59.66   -4.82   -0.82  -33.87   -1.04
198   59.66    216.38  -3.67    1.79  -16.51   -0.62
199   -4.82    -3.67   48.89    4.12  -15.52   -3.59
200   -0.82     1.79    4.12   26.54   -3.60   -6.41
201  -33.87   -16.51  -15.52   -3.60   22.85   -1.67
202   -1.04    -0.62   -3.59   -6.41   -1.67   78.29
```

203 defines the elastic stiffness tensor in GPa of Talc. This example will be discussed in greater  
 204 detail in section 3.2.

## 205 2.3 Crystal Orientations

206 Let  $\vec{X}^c, \vec{Y}^c, \vec{Z}^c$  be a Euclidean crystal coordinate system assigned to a specific crystal and let  
 207  $\vec{X}^s, \vec{Y}^s, \vec{Z}^s$  a specimen coordinate system. Then in general, in polycrystalline materials the  
 208 two coordinate systems do not coincide. Their relative alignment describes the orientation  
 209 of the crystal within the specimen. More specifically, the *orientation* of a crystal is defined

210 as the (active) rotation  $g$  that rotates the specimen coordinate system into coincidence with  
 211 the crystal coordinate system. From another point of view, the rotation  $g$  can be described  
 212 as the basis transformation from the crystal coordinate system to specimen coordinate  
 213 system. Let  $\vec{h} = (h_1, h_2, h_3)$  be the coordinates of a specific direction with respect to the  
 214 crystal coordinate system. Then  $\vec{r} = (r_1, r_2, r_3) = g\vec{h}$  are the coordinates of the same  
 215 direction with respect to the specimen coordinate system.

216 Crystal orientations are typically defined by Euler angles, either by specifying rotations  
 217 with angles  $\phi_1, \Phi, \phi_2$  about the axes  $Z^s, X^s, Z^s$  (Bunge convention), or with angles  $\alpha, \beta, \gamma$   
 218 about the axes  $Z^s, Y^s, Z^s$  (Matthies convention). In MTEX both conventions, and also some  
 219 others, are supported. In order to define an orientation in MTEX we start by fixing the  
 220 crystal reference frame  $\vec{X}^c, \vec{Y}^c, \vec{Z}^c$  used for the definition of the orientation,

```
221 | cs_orientation = symmetry( 'triclinic', [5.29, 9.18, 9.42], [90.4, 98.9, 90.1]*degree, ...
222 | 'X||a', 'Z||c*', 'mineral', 'Talc');
```

```
223 | cs_orientation = crystal symmetry (size: 1)
224 |
225 | mineral           : Talc
226 | symmetry          : triclinic (-1)
227 | a, b, c           : 5.3, 9.2, 9.4
228 | alpha, beta, gamma: 90.4, 98.9, 90.1
229 | reference frame   : X||a, Z||c*
```

230 Now an orientation can be defined as a variable of type `orientation`,

```
231 | g = orientation( 'Euler', 10*degree, 20*degree, 5*degree, 'Bunge', cs_orientation)
```

```
232 | g = orientation (size: 1 1)
233 | mineral           : Talc
234 | crystal symmetry : triclinic, X||a, Z||c*
235 | specimen symmetry: triclinic
236 |
237 | Bunge Euler angles in degree
238 | phi1  Phi phi2
239 | 10    20    5
```

240 Note, that for the definition of an orientation the crystal reference frame is crucial. There-  
 241 fore, the definition of the variable of type `orientation` necessarily includes a variable of  
 242 type `symmetry`, storing the relevant information. This applies, in particular, if the orienta-  
 243 tion data, i.e. Euler angles, are imported from third party measurement systems, such as  
 244 EBSD, and associated software with their own specific conventions for  $\vec{X}^c, \vec{Y}^c, \vec{Z}^c$ , which  
 245 should be defined when using the MTEX import wizard.

246 In order to demonstrate the coordinate transform between the crystal and the specimen  
 247 coordinate system, we choose a crystal direction in the reciprocal lattice  $\vec{h} = h\vec{a}^* + k\vec{b}^* + l\vec{c}^*$   
 248 (pole to a plane) by defining a variable of type `Miller`

```
249 | h = Miller(1,1,0, cs_orientation, 'hkl')
```

```
250 | h = Miller (size: 1 1)
251 | mineral: Talc (triclinic, X||a, Z||c*)
```



```

252 | h 1
253 | k 1
254 | l 0

```

and express it in terms of the specimen coordinate system for a specific orientation  $g = (10^\circ, 20^\circ, 5^\circ)$

```

257 | r = g * h

```

```

258 | r = vector3d (size: 1 1),
259 |           x           y           z
260 | 0.714153  0.62047  0.324041

```

The resulting variable is of type `vector3d` reflecting that the new coordinate system is the specimen coordinate system. Note, that in order that the coordinate transformation rule makes sense physically, the corresponding crystal reference frames used for the definition of the orientation and the crystal direction by Miller indices must coincide. Alternatively, one can specify a crystal direction  $\vec{u} = u\vec{a} + v\vec{b} + w\vec{c}$  in direct space

```

266 | u = Miller (1,1,0, cs_orientation, 'uvw')

```

```

267 | u = Miller (size: 1 1), uvw
268 | mineral: Talc (triclinic, X||a, Z||c*)
269 | u 1
270 | v 1
271 | w 0

```

and express it in terms of the specimen coordinate system

```

273 | r = g * u

```

```

274 | r = vector3d (size: 1 1),
275 |           x           y           z
276 | 0.266258  0.912596  0.310283

```

Obviously, this gives a different direction, since direct and reciprocal space do not coincide for triclinic crystal symmetry.

## 2.4 The relationship between the single crystal physical property and Euler angle reference frames

Let us consider a rank  $r$  tensor  $T_{i_1, \dots, i_r}$  describing some physical property of a crystal with respect to a well defined crystal reference frame  $\vec{X}^T, \vec{Y}^T, \vec{Z}^T$ . Then one is often interested in expressing the tensor with respect to another, different Euclidean reference frame  $\vec{X}, \vec{Y}, \vec{Z}$ , which might be

1. a crystallographically equivalent crystal reference frame,
2. a different convention for aligning the Euclidean reference frame to the crystal coordinate system, or,

3. a specimen coordinate system.

Let us first consider a vector  $\vec{h}$  that has the representation

$$\vec{h} = h_1^T \vec{X}^T + h_2^T \vec{Y}^T + h_3^T \vec{Z}^T$$

with respect to the tensor reference frame  $\vec{X}^T, \vec{Y}^T, \vec{Z}^T$ , and the representation

$$\vec{h} = h_1 \vec{X} + h_2 \vec{Y} + h_3 \vec{Z}.$$

with respect to the other reference frame  $\vec{X}, \vec{Y}, \vec{Z}$ . Then the coordinates  $h_1^T, h_2^T, h_3^T$  and  $h_1, h_2, h_3$  satisfy the transformation rule

$$\begin{pmatrix} h_1 \\ h_2 \\ h_3 \end{pmatrix} = \underbrace{\begin{pmatrix} \vec{X} \cdot \vec{X}^T & \vec{X} \cdot \vec{Y}^T & \vec{X} \cdot \vec{Z}^T \\ \vec{Y} \cdot \vec{X}^T & \vec{Y} \cdot \vec{Y}^T & \vec{Y} \cdot \vec{Z}^T \\ \vec{Z} \cdot \vec{X}^T & \vec{Z} \cdot \vec{Y}^T & \vec{Z} \cdot \vec{Z}^T \end{pmatrix}}_{=:R} \begin{pmatrix} h_1^T \\ h_2^T \\ h_3^T \end{pmatrix}, \quad (1)$$

i.e., the matrix  $R$  performs the coordinate transformation from the tensor reference frame  $\vec{X}^T, \vec{Y}^T, \vec{Z}^T$  to the other reference frame  $\vec{X}, \vec{Y}, \vec{Z}$ . The matrix  $R$  can be also interpreted as the rotation matrix that rotates the second reference frame into coincidence with the tensor reference frame. Considering  $h_j^T$  to be a rank one tensor, the transformation rule becomes

$$h_i = h_j^T R_{ij}.$$

This formula generalizes to arbitrary tensors. Let  $T_{i_1, \dots, i_r}^T$  be the coefficients of a rank  $r$  tensor with respect to the crystal reference frame  $\vec{X}^T, \vec{Y}^T, \vec{Z}^T$  and let  $T_{i_1, \dots, i_r}$  be the coefficients with respect to another reference frame  $X, Y, Z$ . Then the linear orthogonal transformation law for Cartesian tensors states the relationship

$$T_{i_1, \dots, i_r} = T_{j_1, \dots, j_r}^T R_{i_1 j_1} \cdots R_{i_r j_r}. \quad (2)$$

Let us now examine the three cases for a new reference frame as mentioned at the beginning of this section. In the case of a crystallographically equivalent reference frame the coordinate transform  $R$  is a symmetry element of the crystal and the tensor remains invariant with respect to this coordinate transformation, i.e.  $\tilde{T}_{i_1, \dots, i_r} = T_{i_1, \dots, i_r}$ .

In the case that the other reference frame  $\vec{X}, \vec{Y}, \vec{Z}$  follows a different convention in aligning to the crystal coordinate system the transformed tensor  $\tilde{T}_{i_1, \dots, i_r}$  is in general different to the original one. In MTEX this change of reference frame is done by the command `set`. Let us consider the elastic stiffness tensor  $C_{ijkl}$  of Talc as defined above

```

297 C = elastic stiffness tensor (size: 3 3 3 3)
298     unit: GPa
299     rank: 4
300     mineral: Talc (triclinic, X||a*, Z||c)
301
302 219.83    59.66   -4.82   -0.82  -33.87   -1.04

```

```

303 59.66 216.38 -3.67 1.79 -16.51 -0.62
304 -4.82 -3.67 48.89 4.12 -15.52 -3.59
305 -0.82 1.79 4.12 26.54 -3.60 -6.41
306 -33.87 -16.51 -15.52 -3.60 22.85 -1.67
307 -1.04 -0.62 -3.59 -6.41 -1.67 78.29

```

and let us consider the reference frame `cs_orientation` as defined in the previous section

```

309 cs_orientation = Symmetry (size: 1)
310 mineral          : Talc
311 symmetry         : triclinic (-1)
312 a, b, c          : 5.29, 9.18, 9.42
313 alpha, beta, gamma: 90.4, 98.9, 90.1
314 reference frame  : X||a, Z||c*

```

Then the elastic stiffness tensor  $\tilde{C}_{ijkl}$  of Talc with respect to the reference frame `cs_orientation` is computed by setting `cs_orientation` as the new reference frame

```

317 C_orientation = set(C, 'CS', cs_orientation)

```

```

318 C_orientation = elastic stiffness tensor (size: 3 3 3 3)
319   unit: GPa
320   rank: 4
321 mineral: Talc (triclinic, X||a, Z||c*)
322
323 tensor in Voigt matrix representation
324 231.82 63.19 -5.76 0.76 -4.31 -0.59
325 63.19 216.31 -7.23 2.85 -5.99 -0.86
326 -5.76 -7.23 38.92 2.23 -16.69 -4.3
327 0.76 2.85 2.23 25.8 -4.24 1.86
328 -4.31 -5.99 -16.69 -4.24 21.9 -0.14
329 -0.59 -0.86 -4.3 1.86 -0.14 79.02

```

Finally, we consider the case that the second reference frame is not aligned to the crystal coordinate system, but to the specimen coordinate system. Then, according to the previous section, the coordinate transform defines the orientation  $g$  of the crystal and equation (2) tells us how the tensor has to be rotated according to the crystal orientation. In this case we will write

$$T_{i_1, \dots, i_r} = T_{j_1, \dots, j_r}^T(g) = T_{j_1, \dots, j_r}^T R_{i_1 j_1}(g) \cdots R_{i_r j_r}(g), \quad (3)$$

to express the dependency of the resulting tensor from the orientation  $g$ . Here  $R_{i_r j_r}(g)$  is the rotation matrix defined by the orientation  $g$ . It is of major importance, in order to apply formula (3), that both, the tensor reference frame and the crystal reference frame used for describing the orientation coincide. If they do not coincide, the tensor has to be transformed to the same crystal reference frame used for describing the orientation. Hence, when working with tensors and orientation data it is always necessary to know the tensor reference frame and the crystal reference frame used for describing the orientation. In practical applications this is not always a simple task, as those information are sometimes hidden by the commercial EBSD systems.

339 If the corresponding reference frames are specified in the definition of the tensor as  
340 well as in the definition of the orientation, MTEX automatically checks for coincidence and  
341 performs the necessary coordinate transforms if they do not coincide. Eventually, the  
342 rotated tensor for an orientation  $g = (10^\circ, 20^\circ, 5^\circ)$  is computed by the command `rotate`,

```
343 C_rotated = rotate(C,g)
```

```
344 C_rotated = elastic_stiffness tensor (size: 3 3 3 3)  
345 unit: GPa  
346 rank: 4  
347  
348 tensor in Voigt matrix representation  
349 228.79 56.05 1.92 19.99 -13.82 6.85  
350 56.05 176.08 11.69 50.32 -7.62 4.42  
351 1.92 11.69 43.27 5.28 -19.48 2.33  
352 19.99 50.32 5.28 43.41 -1.74 0.24  
353 -13.82 -7.62 -19.48 -1.74 29.35 17.34  
354 6.85 4.42 2.33 0.24 17.34 73.4
```

355 Note, that the resulting tensor does not contain any information on the original mineral  
356 or reference frame. This is because the single crystal tensor is now with respect to the  
357 specimen coordinate system and can be averaged with any other elastic stiffness tensor  
358 from any other crystal of any composition and orientation.

## 359 3 Single crystal anisotropic properties

360 Next we present some classical properties of single crystals that can be described by tensors  
361 (cf. Nye, 1985).

### 362 3.1 Second Rank Tensors

363 A typical second rank tensor describes the relationship between an applied vector field  
364 and an induced vector field, such that the induced effect is equal to the tensor property  
365 multiplied by the applied vector. Examples of such a tensor are

- 366 • the electrical conductivity tensor, where the applied electric field induces a field of  
367 current density,
- 368 • the dielectric susceptibility tensor, where the applied electric field intensity induces  
369 electric polarization,
- 370 • the magnetic susceptibility tensor, where the applied magnetic field induces the in-  
371 tensity of magnetization,
- 372 • the magnetic permeability tensor, where the applied magnetic field induces magnetic  
373 induction,

- the thermal conductivity tensor, where the applied negative temperature gradient induces heat flux.

As a typical example for a second rank tensor we consider the thermal conductivity tensor  $k$ ,

$$k = \begin{pmatrix} k_{11} & k_{12} & k_{13} \\ k_{21} & k_{22} & k_{23} \\ k_{31} & k_{32} & k_{33} \end{pmatrix} = \begin{pmatrix} -\frac{\partial x_1}{\partial T} q_1 & -\frac{\partial x_2}{\partial T} q_1 & -\frac{\partial x_3}{\partial T} q_1 \\ -\frac{\partial x_1}{\partial T} q_2 & -\frac{\partial x_2}{\partial T} q_2 & -\frac{\partial x_3}{\partial T} q_2 \\ -\frac{\partial x_1}{\partial T} q_3 & -\frac{\partial x_2}{\partial T} q_3 & -\frac{\partial x_3}{\partial T} q_3 \end{pmatrix}$$

which relates the negative temperature gradient  $-\text{grad}T = -(\frac{\partial T}{\partial x_1}, \frac{\partial T}{\partial x_2}, \frac{\partial T}{\partial x_3})$  with the heat flux  $q = (q_1, q_2, q_3)$  per unit area by

$$q_i = -\sum_{j=1}^3 k_{ij} \frac{\partial T}{\partial x_j} = -k_{ij} \frac{\partial T}{\partial x_j}. \quad (4)$$

In the present example the applied vector is the negative temperature gradient and the induced vector is the heat flux. Furthermore, we see that the relating vector is built up as a matrix, where the applied vector is the denominator of the rows and the induced vector is the numerator of columns. We see that the tensor entries  $k_{ij}$  describe the heat flux  $q_i$  in direction  $X_i$  given a thermal gradient  $\frac{\partial T}{\partial x_j}$  in direction  $X_j$ .

As an example we consider the thermal conductivity of monoclinic orthoclase (Hofer and Schilling, 2002). We start by defining the tensor reference frame and the tensor coefficients in  $Wm^{-1}K^{-1}$ .

```

384 cs_tensor = symmetry( 'monoclinic', [8.561, 12.996, 7.192], [90, 116.01, 90]*degree, ...
385                      'mineral', 'orthoclase', 'Y||b', 'Z||c');
386
387 M = [[1.45 0.00 0.19];...
388      [0.00 2.11 0.00];...
389      [0.19 0.00 1.79]];

```

Now the thermal conductivity tensor  $k$  is defined by

```

391 k = tensor(M, 'name', 'thermal_conductivity', 'unit', 'W_1/m_1/K', cs_tensor)

```

```

392 k = thermal conductivity tensor (size: 3 3)
393 unit   : W 1/m 1/K
394 rank   : 2
395 mineral: orthoclase (monoclinic, X||a*, Y||b, Z||c)
396
397 1.45    0 0.19
398    0 2.11    0
399 0.19    0 1.79

```

Using the thermal conductivity tensor  $k$  we can compute the thermal flux  $q$  in  $Wm^{-2}$  for a temperature gradient in  $Km^{-1}$

```

402 gradT = Miller(1,1,0, cs_tensor, 'uvw')

```

```

403 gradT = Miller (size: 1 1), uvw
404 mineral: Orthoclase (monoclinic, X||a*, Y||b, Z||c)
405 u 1
406 v 1
407 w 0

```

408 by equation (4), which becomes in MTEX

```

409 q = EinsteinSum(k,[1 -1],gradT,-1,'name','thermal_flux','unit','W_1/m^2')

```

```

410 q = thermal flux tensor (size: 3)
411 unit : W 1/m^2
412 rank : 1
413 mineral: orthoclase (monoclinic, X||a*, Y||b, Z||c)
414
415 0.672
416 1.7606
417 -0.3392

```

418 Note that the  $-1$  in the arguments of the command `EinsteinSum` indicates the dimension  
419 which has to be summed up and the  $1$  in the argument indicates that the first dimension  
420 of  $k$  becomes the first dimension of  $q$ , see equation (4)

A second order tensor  $k_{ij}$  can be visualized by plotting its magnitude  $R(\vec{x})$  in a given direction  $\vec{x}$ ,

$$R(\vec{x}) = k_{ij}\vec{x}_i\vec{x}_j.$$

421 In MTEX the magnitude in a given direction  $\vec{x}$  can be computed via

```

422 x = Miller(1,0,0,cs_tensor,'uvw');
423
424 R = EinsteinSum(k,[-1 -2],x,-1,x,-2)

```

```

425 R = tensor (size: )
426 rank : 0
427 mineral: orthoclase (monoclinic, X||a*, Y||b, Z||c)
428
429 1.3656

```

430 Again the negative arguments  $-1$  and  $-2$  indicates which dimensions have to be multiplied  
431 and summed up. Alternatively, one can use the command `magnitude`,

```

432 R = directionalMagnitude(k,x)

```

433 Since in MTEX the directional magnitude is the default output of the `plot` command, the  
434 code

```

435 plot(k)
436 colorbar

```

437 plots the directional magnitude of  $k$  with respect to any direction  $\vec{x}$  as shown in Figure  
438 1. Note that, by default, the  $X$  axis is plotted in north direction, the  $Y$  is plotted in  
439 west direction, and the  $Z$  axis is at the center of the plot. This default alignment can be  
440 changed by the commands `plotx2north`, `plotx2east`, `plotx2south`, `plotx2west`.

441 When the tensor  $k$  is rotated the directional magnitude rotates accordingly. This can  
 442 be checked in MTEX by

```
443 g = orientation('Euler',10*degree,20*degree,30*degree,cs_tensor);
444 k_rot = rotate(k,g);
445 plot(k_rot)
```

446 The resulting plot is shown in Figure 1.

447 From the directional magnitude we observe, furthermore, that the thermal conductivity  
 448 tensor  $k$  is symmetric, i.e.,  $k_{ij} = k_{ji}$ . This implies, in particular, that the thermal conduc-  
 449 tivity is an *axial* or *non-polar* property, which means that the magnitude of heat flow is  
 450 the same in positive or negative crystallographic directions.

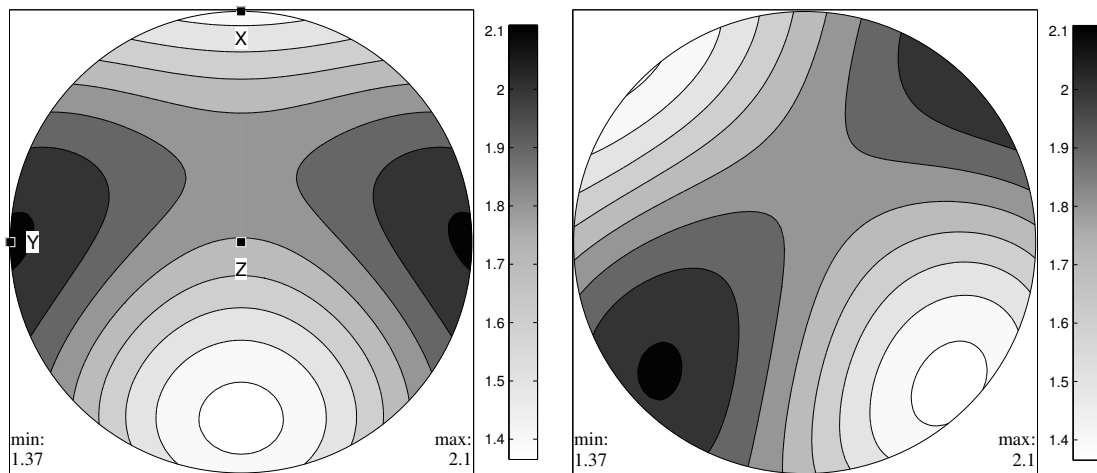


Figure 1: The thermal conductivity  $k$  of Orthoclase visualized by its directionally varying magnitude for the tensor in standard orientation (left plot) and for the rotated tensor (right plot).

We want to emphasize that there are also second rank tensors, which do not describe the relationship between an applied vector field and an induced vector field, but relates, for instance, a zero rank tensor to a second rank tensor. The thermal expansion tensor  $\alpha$ ,

$$\alpha_{ij} = \frac{\partial \varepsilon_{ij}}{\partial T},$$

is an example of such a tensor which relates a small applied temperature change  $\partial T$ , which is a scalar, i.e., a zero rank tensor, to the induced strain tensor  $\varepsilon_{ij}$ , which is a second rank tensor. The corresponding coefficient of volume thermal expansion becomes

$$\frac{1}{V} \frac{\partial V}{\partial T} = \alpha_{ii}.$$

451 This relationship holds true only for small changes in temperature. For larger changes in  
 452 temperature, higher order terms have to be considered (see Fei, 1995 for data on minerals).  
 453 This also applies to other tensors.

### 3.2 Elasticity Tensors

We will now present fourth rank tensors, but restrict ourselves to the elastic tensors. Let  $\sigma_{ij}$  be the second rank stress tensor and let  $\varepsilon_{kl}$  be the second rank infinitesimal strain tensor. Then the fourth rank elastic stiffness tensor  $C_{ijkl}$  describes the stress  $\sigma_{ij}$  induced by the strain  $\varepsilon_{kl}$ , i.e., it is defined by the equality

$$\sigma_{ij} = C_{ijkl}\varepsilon_{kl}, \quad (5)$$

which is known as Hooke's law for linear elasticity. Alternatively, the fourth order elastic compliance tensor  $S_{ijkl}$  describes the strain  $\varepsilon_{kl}$  induced by the stress  $\sigma_{ij}$ , i.e., it is defined by the equality

$$\varepsilon_{kl} = S_{ijkl}\sigma_{ij}.$$

The above definitions may also be written as the equalities

$$C_{ijkl} = \frac{\partial \sigma_{ij}}{\partial \varepsilon_{kl}} \quad \text{and} \quad S_{ijkl} = \frac{\partial \varepsilon_{kl}}{\partial \sigma_{ij}}.$$

In the case of static equilibrium for the stress tensor and infinitesimal deformation for the strain tensor, both tensors are symmetric, i.e.,  $\sigma_{ij} = \sigma_{ji}$  and  $\varepsilon_{ij} = \varepsilon_{ji}$ . This implies for the elastic stiffness tensor the symmetry

$$C_{ijkl} = C_{ijlk} = C_{jikl} = C_{jilk},$$

reducing the number of independent entries of the tensor from  $3^4 = 81$  to 36. Since, the elastic stiffness  $C_{ijkl}$  is related to the internal energy  $U$  of a body, assuming constant entropy, by

$$C_{ijkl} = \frac{\partial}{\partial \varepsilon_{kl}} \left( \frac{\partial U}{\partial \varepsilon_{ij}} \right),$$

we obtain by Schwarz integrability condition

$$C_{ijkl} = \frac{\partial}{\partial \varepsilon_{kl}} \left( \frac{\partial U}{\partial \varepsilon_{ij}} \right) = \left( \frac{\partial^2 U}{\partial \varepsilon_{ij} \partial \varepsilon_{kl}} \right) = \left( \frac{\partial^2 U}{\partial \varepsilon_{kl} \partial \varepsilon_{ij}} \right) = C_{klij}.$$

Hence,

$$C_{ijkl} = C_{klij},$$

which further reduces the number of independent entries from 36 to 21 ( e.g. Mainprice, 2007). These 21 independent entries may be efficiently represented in from of a symmetric  $6 \times 6$  matrix  $C_{mn}$ ,  $m, n = 1, \dots, 6$  as introduced by Voigt (1928). The entries  $C_{mn}$  of this matrix representation equal the tensor entries  $C_{ijkl}$  whenever  $m$  and  $n$  correspond to  $ij$  and  $kl$  according to the following table.

$m$ or $n$	1	2	3	4	5	6
$ij$ or $kl$	11	22	33	23, 32	13, 31	12, 21



455 The Voigt notation is used for published compilations of elastic tensors (e.g. Bass, 1995,  
456 Isaak, 2001).

In a similar manner a Voigt representation  $S_{mn}$  is defined for the elastic compliance tensor  $S_{ijkl}$ . However, there are additional factors when converting between the Voigt  $S_{mn}$  matrix representation and the tensor representation  $S_{ijkl}$ . More precisely, we have for all  $ij, kl, m, n$  which correspond to each other according to the above table the identities:

$$S_{ijkl} = P \cdot S_{mn}, \quad \begin{cases} P = 1, & \text{if both } m, n = 1, 2, 3 \\ P = \frac{1}{2}, & \text{if either } m \text{ or } n \text{ are } 4, 5, 6 \\ P = \frac{1}{4}, & \text{if both } m, n = 4, 5, 6 \end{cases}$$

Using the Voigt matrix representation of the elastic stiffness tensor equation (5) may be written as

$$\begin{pmatrix} \sigma_{11} \\ \sigma_{22} \\ \sigma_{33} \\ \sigma_{23} \\ \sigma_{13} \\ \sigma_{12} \end{pmatrix} = \begin{pmatrix} C_{11} & C_{12} & C_{13} & C_{14} & C_{15} & C_{16} \\ C_{21} & C_{22} & C_{23} & C_{24} & C_{25} & C_{26} \\ C_{31} & C_{32} & C_{33} & C_{34} & C_{35} & C_{36} \\ C_{41} & C_{42} & C_{43} & C_{44} & C_{45} & C_{46} \\ C_{51} & C_{52} & C_{53} & C_{54} & C_{55} & C_{56} \\ C_{61} & C_{62} & C_{63} & C_{64} & C_{65} & C_{66} \end{pmatrix} \begin{pmatrix} \varepsilon_{11} \\ \varepsilon_{22} \\ \varepsilon_{33} \\ 2\varepsilon_{23} \\ 2\varepsilon_{13} \\ 2\varepsilon_{12} \end{pmatrix}.$$

457 The matrix representation of Hooke's law allows for a straightforward interpretation of the  
458 tensor coefficients  $C_{ij}$ . E.g., the tensor coefficient  $C_{11}$  describes the dependency between  
459 normal stress  $\sigma_{11}$  in direction  $X$  and axial strain  $\varepsilon_{11}$  in the same direction. The coefficient  
460  $C_{14}$  describes the dependency between normal stress  $\sigma_{11}$  in direction  $X$  and shear strain  
461  $2\varepsilon_{23} = 2\varepsilon_{32}$  in direction  $Y$  in the plane normal to  $Z$ . The dependency between normal  
462 stress  $\sigma_{11}$  and axial strains  $\varepsilon_{11}, \varepsilon_{22}, \varepsilon_{33}$ , along  $X, Y$  and  $Z$  is described by  $C_{11}, C_{12}$  and  $C_{13}$ ,  
463 whereas the dependencies between the normal stress  $\sigma_{11}$  and shear strains  $2\varepsilon_{23}, 2\varepsilon_{13}$  and  
464  $2\varepsilon_{12}$  are described by  $C_{14}, C_{15}$  and  $C_{16}$ . These effects are most important in low symmetry  
465 crystals, such as triclinic and monoclinic crystals, where there are a large number of non-  
466 zero coefficients.

467 In MTEX the elasticity tensors may be specified directly in Voigt notation as we have  
468 already seen in Section 2.2. Alternatively, tensors may also be imported from ASCII files  
469 using a graphical interface called `import_wizard` in MTEX.

470 Let  $\mathbf{C}$  be the elastic stiffness tensor for Talc in GPa as defined in Section 2.2.

```
471 C = elastic_stiffness tensor (size: 3 3 3 3)
472 unit : GPa
473 rank : 4
474 mineral: Talc (triclinic, X||a*, Z||c)
475
476 tensor in Voigt matrix representation
477 219.83 59.66 -4.82 -0.82 -33.87 -1.04
478 59.66 216.38 -3.67 1.79 -16.51 -0.62
479 -4.82 -3.67 48.89 4.12 -15.52 -3.59
480 -0.82 1.79 4.12 26.54 -3.6 -6.41
481 -33.87 -16.51 -15.52 -3.6 22.85 -1.67
482 -1.04 -0.62 -3.59 -6.41 -1.67 78.29
```

483 Then the elastic compliance  $S$  in  $\text{GPa}^{-1}$  can be computed by inverting the tensor  $C$ .

484 `S = inv(C)`

```
485 S = elastic compliance tensor (size: 3 3 3 3)
486 unit : 1/GPa
487 rank : 4
488 mineral: Talc (triclinic, X||a*, Z||c)
489
490 tensor in Voigt matrix representation
491 0.00691 -0.000834 0.004712 0.000744 0.006563 0.000352
492 -0.000834 0.005139 0.001413 -4.4e-05 0.001717 8e-05
493 0.004712 0.001413 0.030308 -0.000133 0.014349 0.001027
494 0.000744 -4.4e-05 -0.000133 0.009938 0.002119 0.000861
495 0.006563 0.001717 0.014349 0.002119 0.021706 0.001016
496 0.000352 8e-05 0.001027 0.000861 0.001016 0.003312
```

### 497 3.3 Elastic Properties

498 The fourth order elastic stiffness tensor  $C_{ijkl}$  and fourth order elastic compliance tensor  
499  $S_{ijkl}$  are the starting point for the calculation of a number of elastic anisotropic physical  
500 properties, which include

- 501 • Young's modulus,
- 502 • shear modulus,
- 503 • Poisson's ratio,
- 504 • linear compressibility,
- 505 • compressional and shear elastic wave velocities,
- 506 • wavefront velocities,
- 507 • mean sound velocities,
- 508 • Debye temperature,

509 and, of course, of their isotropic equivalents. In the following we shall give a short overview  
510 over these properties.

**Scalar volume compressibility.** First we consider the *scalar volume compressibility*  $\beta$ . Using the fact that the change of volume is given in terms of the strain tensor  $\varepsilon_{ij}$  by

$$\frac{\partial V}{V} = \varepsilon_{ii},$$

we derive for hydrostatic or isotropic pressure, which is given by the stress tensor  $\sigma_{kl} = -P\delta_{kl}$ , that the change of volume is given by

$$\frac{\partial V}{V} = -PS_{iikk}.$$

Hence, the volume compressibility is

$$\beta = -\frac{\partial V}{V} \frac{1}{P} = S_{iikk}.$$

**Linear compressibility.** The *linear compressibility*  $\beta(x)$  of a crystal is the strain, i.e. the relative change in length  $\frac{\partial l}{l}$ , for a specific crystallographic direction  $x$ , when the crystal is subjected to a unit change in hydrostatic pressure  $-P\delta_{kl}$ . From

$$\frac{\partial l}{l} = \varepsilon_{ij}x_i x_j = -PS_{iikk}x_i x_j$$

we conclude

$$\beta(x) = -\frac{\partial l}{l} \frac{1}{P} = S_{ijkk}x_i x_j.$$

**Youngs modulus.** The *Young's modulus*  $E$  is the ratio of the axial (longitudinal) stress to the lateral (transverse) strain in a tensile or compressive test. As we have seen earlier when discussing the elastic stiffness tensor, this type of uniaxial stress is accompanied by lateral and shear strains as well as the axial strain. The Young's modulus in direction  $x$  is given by

$$E(x) = (S_{ijkl}x_i x_j x_k x_l)^{-1}.$$

**Shear modulus.** Unlike Young's modulus, the *shear modulus*  $G$  in an anisotropic medium is defined using two directions; the shear plane  $h$  and the shear direction  $u$ . For example, if the shear stress  $\sigma_{12}$  results in the shear strain  $2\varepsilon_{12}$ . Then the corresponding shear modulus is  $G = \frac{\sigma_{12}}{2\varepsilon_{12}}$ . From Hooke's law we have

$$\varepsilon_{12} = S_{1212}\sigma_{12} + S_{1221}\sigma_{21},$$

hence  $G = (4S_{1212})^{-1}$ . The shear modulus for an arbitrary, but orthogonal, shear plane  $h$  and shear direction  $u$  is given by

$$G(h, u) = (4S_{ijkl}h_i u_j h_k u_l)^{-1}$$

511 **Poisson's Ratio.** *Anisotropic Poisson's ratio* is defined by the elastic strain in two or-  
 512 thogonal directions, the longitudinal (or axial) direction  $x$  and the transverse (or lateral)  
 513 direction  $y$ . The lateral strain is defined by  $-\varepsilon_{ij}y_i y_j$  along  $y$  and the longitudinal strain  
 514 by  $\varepsilon_{ij}x_i x_j$  along  $x$ . The anisotropic Poisson's ratio  $\nu(x,y)$  is given as the ratio of lateral to  
 515 longitudinal strain (Sirotnin and Shakolskaya, 1982) as

$$\nu(x, y) = -\frac{\varepsilon_{ij} y_i y_j}{\varepsilon_{kl} x_k x_l} = -\frac{S_{ijkl} x_i x_j y_k y_l}{S_{mnop} x_m x_n x_o x_p}.$$

516 The anisotropic Poisson's ratio has recently been reported for talc (Mainprice et al., 2008)  
 517 and has been found to be negative for many directions at low pressure.

**Wave velocities.** The Christoffel equation, first published by Christoffel (1877), can be used to calculate elastic wave velocities and the polarizations in an anisotropic elastic medium from the elastic stiffness tensor  $C_{ijkl}$ , or, more straightforward, from the Christoffel tensor  $T_{ik}$  which is for a unit propagation direction  $\vec{n}$  defined by

$$T_{ik}(\vec{n}) = C_{ijkl} \vec{n}_j \vec{n}_l.$$

Since the elastic tensors are symmetric, we have

$$T_{ik}(\vec{n}) = C_{ijkl} n_j n_l = C_{jikl} \vec{n}_j \vec{n}_l = C_{ijlk} \vec{n}_j \vec{n}_l = C_{klij} \vec{n}_j \vec{n}_l = T_{ki}(\vec{n}),$$

518 and, hence, the Christoffel tensor  $T(\vec{n})$  is symmetric. The Christoffel tensor is also invariant  
 519 upon the change of sign of the propagation direction as the elastic tensor is not sensitive to  
 520 the presence or absence of a center of crystal symmetry, being a centro-symmetric physical  
 521 property.

Because the elastic strain energy  $1/2 C_{ijkl} \varepsilon_{ij} \varepsilon_{kl}$  of a stable crystal is always positive and real (e.g. Nye, 1985), the eigenvalues  $\lambda_1, \lambda_2, \lambda_3$  of the Christoffel tensor  $T_{ik}(\vec{n})$  are real and positive. They are related to the wave velocities  $V_p, V_{s1}$  and  $V_{s2}$  of the plane P-, S1- and S2-waves propagating in the direction  $\vec{n}$  by the formulae

$$V_p = \sqrt{\frac{\lambda_1}{\rho}}, \quad V_{s1} = \sqrt{\frac{\lambda_2}{\rho}}, \quad V_{s2} = \sqrt{\frac{\lambda_3}{\rho}},$$

522 where  $\rho$  denotes the material density. The three eigenvectors of the Christoffel tensor  
 523 are the polarization directions, also called vibration, particle movement or displacement  
 524 vectors, of the three waves. As the Christoffel tensor is symmetric the three polarization  
 525 directions are mutually perpendicular. In the most general case there are no particular  
 526 angular relationships between polarization directions  $p$  and the propagation direction  $\vec{n}$ .  
 527 However, typically, the P-wave polarization direction is nearly parallel and the two S-waves  
 528 polarizations are nearly perpendicular to the propagation direction. They are termed quasi-  
 529 P or quasi-S waves. The S wave velocities may be identified unambiguously by their relative  
 530 velocity  $V_{s1} > V_{s2}$ .

531 All the elastic properties mentioned in this section have direct expressions in MTEX, i.e.,  
 532 there are the commands

```
533 | beta = volumeCompressibility(C)
534 | beta = linearCompressibility(C, x)
535 | E = YoungsModulus(C, x)
536 | G = shearModulus(C, h, u)
537 | nu = PoissonRatio(C, x, y)
538 | T = ChristoffelTensor(C, n)
```

539 Note, that all these commands take the compliance tensor  $C$  as basis for the calculations.  
 540 For the calculation of the wave velocities the command `velocity`

```
541 [vp, vs1, vs2, pp, ps1, ps2] = velocity(C, x, rho)
```

542 allows for the computation of the wave velocities and the corresponding polarization di-  
 543 rections.

### 544 3.4 Visualization

545 In order to visualize the above quantities, MTEX offers a simple, yet flexible, syntax. Let us  
 546 demonstrate it using the Talc example of the previous section. In order to plot the linear  
 547 compressibility  $\beta(\vec{x})$  or Young's Modulus  $E(\vec{x})$  as a function of the direction  $\vec{x}$  one uses  
 548 the commands

```
549 plot(C, 'PlotType', 'linearCompressibility')  

  550 plot(C, 'PlotType', 'YoungsModulus')
```

551 The resulting plots are shown in Figure 2.

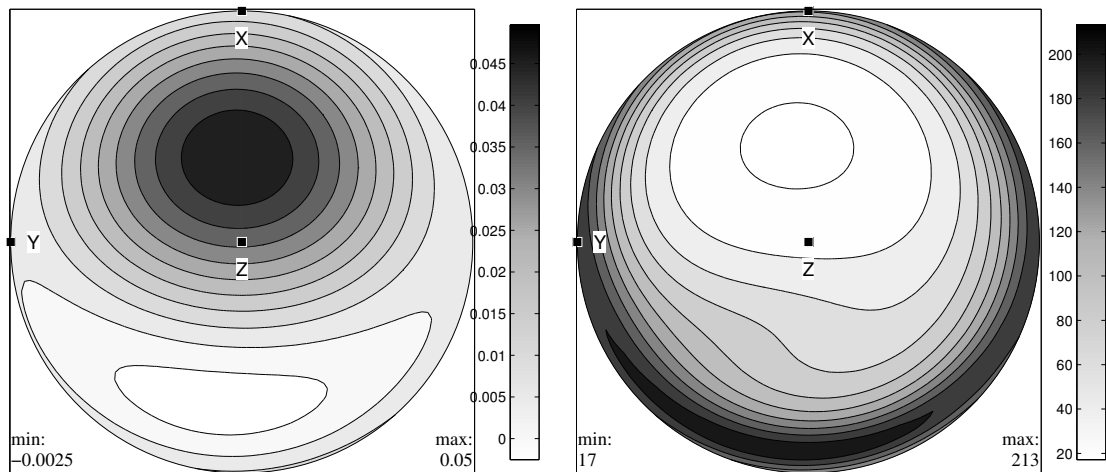


Figure 2: The linear compressibility in  $\text{GPa}^{-1}$  (left plot) and Young's modulus in  $\text{GPa}$  (right plot) for Talc.

552 Next we want to visualize the wave velocities and the polarization directions. Let us  
 553 start with the P-wave velocity in  $\text{kms}^{-1}$  which is plotted by

```
554 rho = 2.78276;  

  555 plot(C, 'PlotType', 'velocity', 'vp', 'density', rho)
```

556 Note that we had to pass the density  $\rho$  in  $\text{gcm}^{-3}$  to the `plot` command. Next we want to  
 557 add on top of this plot the P-wave polarization directions. Therefore, we use the command  
 558 `hold on` and `hold off` to prevent MTEX from clearing the output window,

```
559 hold on  

  560 plot(C, 'PlotType', 'velocity', 'pp', 'density', rho);  

  561 hold off
```

562 The result is shown in Figure 3. Instead of only specifying the variables to plot, one can  
 563 also perform simple calculations. For example by writing

```
564 plot(C, 'PlotType', 'velocity', '200*(vs1-vs2)./(vs1+vs2)', 'density', rho);
565 hold on
566 plot(C, 'PlotType', 'velocity', 'ps1', 'density', rho);
567 hold off
```

568 the S-wave anisotropy in percent is plotted together with the polarization directions of  
 569 the fastest S-wave `ps1`. Another example illustrating the flexibility of the system is the  
 570 following plot of the velocity ratio  $V_p/V_{s1}$  together with the S1-wave polarizations direction.

```
571 plot(C, 'PlotType', 'velocity', 'vp./vs1', 'density', rho);
572 hold on
573 plot(C, 'PlotType', 'velocity', 'ps1', 'density', rho);
574 hold off
```

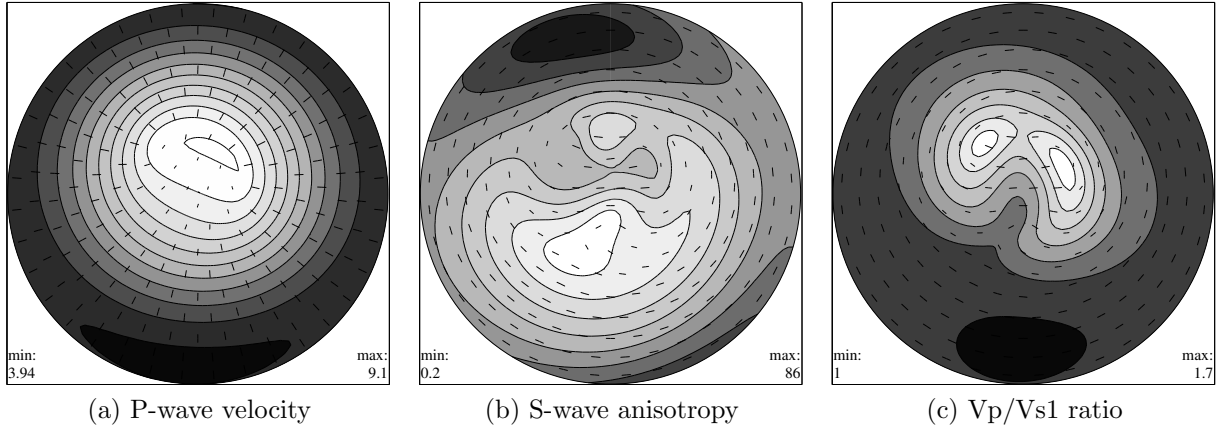


Figure 3: Wave velocities of a Talc crystal. Figure (a) shows the P-wave velocity together with the P-wave polarization direction. Figure (b) shows the S-wave anisotropy in percent together with the S1-wave polarization direction, whereas Figure (c) shows the ratio of  $V_p/V_{s1}$  velocities together with the S1-wave polarization direction.

## 575 4 Anisotropic properties of polyphase aggregates

576 In this section we are concerned with the problem of calculating average physical properties  
 577 of polyphase aggregates. To this end two ingredients are required for each phase  $p$ :

- 578 1. the property tensor  $T_{i_1, \dots, i_r}^p$  describing the physical behavior of a single crystal in the  
 579 reference orientation,
- 580 2. the *orientation density function* (ODF)  $f^p(g)$  describing the volume portion  $\frac{\Delta V}{V}$  of  
 581 crystals having orientation  $g$ ,

582 **or**  
 583 a representative set of individual orientations  $g_m$ ,  $m = 1, \dots, M$ , for example mea-  
 584 sured by EBSD.

585 As an example we consider an aggregate composed of two minerals, Glaucofane and  
 586 Epidote using data from a Blue Schist. The corresponding crystal reference frames are  
 587 defined by

```
588 cs_Glaucofane = symmetry( '2/m', [9.5334, 17.7347, 5.3008],
589 [90.00, 103.597, 90.00]*degree, 'mineral', 'Glaucofane ');
590
591 cs_Epidote = symmetry( '2/m', [8.8877, 5.6275, 10.1517],
592 [90.00, 115.383, 90.00]*degree, 'mineral', 'Epidote ');
```

593 For Glaucofane the elastic stiffness was measured by Bezacier et al. (2010) who give the  
 594 tensor

```
595 C_Glaucofane = tensor (size: 3 3 3 3)
596 rank : 4
597 mineral: Glaucofane (2/m, X||a*, Y||b, Z||c)
598
599 tensor in Voigt matrix representation
600 122.28 45.69 37.24 0 2.35 0
601 45.69 231.5 74.91 0 -4.78 0
602 37.24 74.91 254.57 0 -23.74 0
603 0 0 0 79.67 0 8.89
604 2.35 -4.78 -23.74 0 52.82 0
605 0 0 0 8.89 0 51.24
```

606 and for Epidote the elastic stiffness was measured by Aleksandrov et al. (1974) who gives  
 607 the tensor

```
608 C_Epidote = tensor (size: 3 3 3 3)
609 rank : 4
610 mineral: Epidote (2/m, X||a*, Y||b, Z||c)
611
612 tensor in Voigt matrix representation
613 211.5 65.6 43.2 0 -6.5 0
614 65.6 239 43.6 0 -10.4 0
615 43.2 43.6 202.1 0 -20 0
616 0 0 0 39.1 0 -2.3
617 -6.5 -10.4 -20 0 43.4 0
618 0 0 0 -2.3 0 79.5
```

## 619 4.1 Computing the average tensor from individual orientations

620 We start with the case that we have individual orientation data  $g_m$ ,  $m = 1, \dots, M$ , i.e.,  
 621 from EBSD or U-stage measurements, and volume fractions  $V_m$ ,  $m = 1, \dots, M$ . Then  
 622 the best-known averaging techniques for obtaining estimates of the effective properties  
 623 of aggregates are those developed for elastic constants by Voigt (1887,1928) and Reuss

624 (1929). The *Voigt average* is defined by assuming that the induced tensor (in broadest  
625 sense including vectors) field is everywhere homogeneous or constant, i.e., the induced  
626 tensor at every position is set equal to the macroscopic induced tensor of the specimen. In  
627 the classical example of elasticity the strain field is considered constant. The Voigt average  
628 is sometimes called the “series” average by analogy with Ohms law for electrical circuits.

The Voigt average specimen effective tensor  $\langle T \rangle^{\text{Voigt}}$  is defined by the volume average of the individual tensors  $T(g_m^c)$  with crystal orientations  $g_m^c$  and volume fractions  $V_m$ ,

$$\langle T \rangle^{\text{Voigt}} = \sum_{m=1}^M V_m T(g_m^c).$$

Contrarily, the *Reuss average* is defined by assuming that the applied tensor field is every-  
where constant, i.e., the applied tensor at every position is set equal to the macroscopic  
applied tensor of the specimen. In the classical example of elasticity the stress field is  
considered constant. The Reuss average is sometimes called the “parallel” average. The  
specimen effective tensor  $\langle T \rangle^{\text{Reuss}}$  is defined by the volume ensemble average of the in-  
verses of the individual tensors  $T^{-1}(g_m^c)$ ,

$$\langle T \rangle^{\text{Reuss}} = \left[ \sum_{m=1}^M V_m T^{-1}(g_m^c) \right]^{-1}.$$

The experimentally measured tensor of aggregates is in general between the Voigt and  
Reuss average bounds as the applied and induced tensor fields distributions are expected  
to be between uniform induced (Voigt bound) and uniform applied (Reuss bound) field  
limits. Hill (1952) observed that the arithmetic mean of the Voigt and Reuss bounds

$$\langle T \rangle^{\text{Hill}} = \frac{1}{2} \left( \langle T \rangle^{\text{Voigt}} + \langle T \rangle^{\text{Reuss}} \right),$$

629 sometimes called the Hill or Voigt-Reuss-Hill (VRH) average, is often close to experimen-  
630 tal values for the elastic fourth order tensor. Although VRH average has no theoretical  
631 justification, it is widely used in earth and materials sciences.

632 In the example outlined above of an aggregate consisting of Glaucofane and Epidote  
633 we consider an EBSD data set measured by Bezacier et al. (2010). In MTEX such individual  
634 orientation data are represented by a variable of type EBSD which is generated from an  
635 ASCII file containing the individual orientation measurements by the command

```
636 | ebsd = loadEBSD( 'FileName', {cs_Glaucofane, cs_Epidote} )
```

```
637 | ebsd = EBSD (Groix_A50_5_stitched.ctf)
638 |   properties: bands, bc, bs, error, mad
639 |   phase orientations      mineral symmetry   crystal reference frame
640 |     1          155504 Glaucofane          2/m          X||a*, Y||b, Z||c
641 |     2           63694  Epidote            2/m          X||a*, Y||b, Z||c
```



642 It should be noted that for both minerals the crystal reference frames have to be specified  
643 in the command `loadEBSD`.

644 Now, the Voigt, Reuss, and Hill average tensors can be computed for each phase seper-  
645 ately by the command `calcTensor`,

```
646 | [TVoigt, TReuss, THill] = calcTensor(ebsd, C_Epidote, 'phase', 2)
```

```
647 C_Voigt = tensor (size: 3 3 3 3)
648 rank: 4
649
650 tensor in Voigt matrix representation
651 215 55.39 66.15 -0.42 3.02 -4.69
652 55.39 179.04 59.12 1.04 -1.06 0.06
653 66.15 59.12 202.05 0.94 1.16 -0.77
654 -0.42 1.04 0.94 60.67 -0.86 -0.55
655 3.02 -1.06 1.16 -0.86 71.77 -0.65
656 -4.69 0.06 -0.77 -0.55 -0.65 57.81
```

```
657
658 C_Reuss = tensor (size: 3 3 3 3)
659 rank: 4
660
661 tensor in Voigt matrix representation
662 201.17 56.48 65.94 -0.28 3.21 -4.68
663 56.48 163.39 61.49 1.23 -1.58 -0.13
664 65.94 61.49 189.67 1.29 0.75 -0.64
665 -0.28 1.23 1.29 52.85 -0.99 -0.38
666 3.21 -1.58 0.75 -0.99 65.28 -0.6
667 -4.68 -0.13 -0.64 -0.38 -0.6 50.6
```

```
668
669 C_Hill = tensor (size: 3 3 3 3)
670 rank: 4
671
672 tensor in Voigt matrix representation
673 208.09 55.93 66.05 -0.35 3.11 -4.69
674 55.93 171.22 60.31 1.13 -1.32 -0.04
675 66.05 60.31 195.86 1.11 0.96 -0.71
676 -0.35 1.13 1.11 56.76 -0.93 -0.46
677 3.11 -1.32 0.96 -0.93 68.52 -0.62
678 -4.69 -0.04 -0.71 -0.46 -0.62 54.21
```

679 If no phase is specified and all the tensors for all phases are specified the command

```
680 | [TVoigt, TReuss, THill] = calcTensor(ebsd, C_Glaucophane, C_Epidote)
```

681 computes the average over all phases. These calculations have been validated using the  
682 Careware FORTRAN code (Mainprice,1990). We emphasize that MTEX automatically  
683 checks for the agreement of the EBSD and tensor reference frames for all phases. In  
684 case different conventions have been used MTEX automatically transforms the EBSD data  
685 into the convention of the tensors.

## 686 4.2 Computing the average tensor from an ODF

687 Next we consider the case that the texture is given by an ODF  $f$ . The ODF may origi-  
 688 nate from texture modeling (Bachmann *et al.* 2010), pole figure inversion (Hielscher and  
 689 Schaeben, 2008) or density estimation from EBSD data (Hielscher *et al.* 2010). All these  
 690 diverse sources may be handled by MTEX.

The Voigt average  $\langle T \rangle^{\text{Voigt}}$  of a tensor  $T$  given an ODF  $f$  is defined by the integral

$$\langle T \rangle^{\text{Voigt}} = \int_{\text{SO}(3)} T(g) f(g) dg. \quad (6)$$

whereas the Reuss average  $\langle T \rangle^{\text{Reuss}}$  is defined as

$$\langle T \rangle^{\text{Reuss}} = \left[ \int_{\text{SO}(3)} T^{-1}(g) f(g) dg \right]^{-1}. \quad (7)$$

The integrals (6) and (9) can be computed in two different ways. First one can use a quadrature rule, i.e. for a set of orientations  $g_m$  and weights  $\omega_m$  the Voigt average is approximated by

$$\langle T \rangle^{\text{Voigt}} \approx \sum_{m=1}^M T(g_m) \omega_m f(g_m).$$

Clearly, the accuracy of the approximation depends on the number of nodes  $g_m$  and the smoothness of the ODF. An alternative approach to compute the average tensor, that avoids this dependency, uses the expansion of the rotated tensor into generalized spherical harmonics,  $D_{kk'}^\ell(g)$ . Let  $T_{i_1, \dots, i_r}$  be a tensor of rank  $r$ . Then it is well known (cf. Kneer, 1965, Bunge 1968, Ganster and Geiss, 1985, Humbert and Diz, 1991, Mainprice and Humbert, 1994, Morris, 2006) that the rotated tensor  $T_{i_1, \dots, i_r}(g)$  has an expansion into generalized spherical harmonics up to order  $r$ ,

$$T_{i_1, \dots, i_r}(g) = \sum_{\ell=0}^r \sum_{k, k'=-\ell}^{\ell} \hat{T}_{i_1, \dots, i_r}(l, k, k') D_{kk'}^\ell(g). \quad (8)$$

The explicit calculations of the coefficients  $\hat{T}_{i_1, \dots, i_r}(l, k, k')$  are given in Appendix A. Assume that the ODF has an expansion into generalized spherical harmonics of the form

$$f(g) = \sum_{\ell=0}^r \sum_{k, k'=-\ell}^{\ell} \hat{f}(l, k, k') D_{kk'}^\ell(g).$$

Then, the average tensor with respect to this ODF can be computed by the formula

$$\begin{aligned} \frac{1}{8\pi^2} \int_{\text{SO}(3)} T_{i_1, \dots, i_r}(g) f(g) dg &= \frac{1}{8\pi^2} \int_{\text{SO}(3)} T_{i_1, \dots, i_r}(g) \overline{f(g)} dg \\ &= \sum_{\ell=0}^r \frac{1}{2\ell+1} \sum_{k, k'=-\ell}^{\ell} \hat{T}_{i_1, \dots, i_r}(l, k, k') \overline{\hat{f}(l, k, k')}. \end{aligned}$$

691 MTEX by default uses the Fourier approach that is much faster than using numerical  
 692 integration (quadrature rule), which requires a discretization of the ODF. Numerical inte-  
 693 gration is applied only in those cases when MTEX cannot determine the Fourier coefficients  
 694 of the ODF in an efficient manner. At the present time only the Bingham distributed  
 695 ODFs pose this problem. All the necessary calculations are done automatically, including  
 696 the correction for different crystal reference frames.

697 Let us consider once again the aggregate consisting of Glaucofane and Epidote and  
 698 the corresponding EBSD data set as mentioned in Section 4.1. Then we can estimate for  
 699 any phase an ODF by

```
700 | odf_Epidote = calcODF(ebsd, 'phase', 2)
```

```
701 | odf_Epidote = ODF (ODF estimated from Groix_A50_5_stitched.ctf)
702 | mineral           : Epidote
703 | crystal symmetry : 2/m, X||a*, Y||b, Z||c
704 | specimen symmetry: triclinic
705 |
706 | Portion specified by Fourier coefficients:
707 | degree: 28
708 | weight: 1
```

709 Next, we can compute the average tensors directly from the ODF

```
710 | [TVoigt, TReuss, THill] = calcTensor(odf_Epidote, C_Epidote)
```

```
711 | C_Voigt = tensor (size: 3 3 3 3)
712 | rank: 4
713 |
714 | tensor in Voigt matrix representation
715 | 212.64  56.81  65.68 -0.25  2.56   -4
716 | 56.81  179.21  59.64  0.93 -0.83 -0.27
717 | 65.68  59.64  201.3  0.87  1.12 -0.71
718 | -0.25  0.93  0.87  61.33 -0.79 -0.35
719 | 2.56  -0.83  1.12 -0.79  71.1 -0.48
720 | -4  -0.27 -0.71 -0.35 -0.48  59.29
```

```
721 |
722 | C_Reuss = tensor (size: 3 3 3 3)
723 | rank: 4
724 |
725 | tensor in Voigt matrix representation
726 | 197.91  57.92  65.4 -0.09  2.53   -4
727 | 57.92  163.68  61.84  1.13 -1.27 -0.4
728 | 65.4  61.84  188.53  1.21  0.7 -0.58
729 | -0.09  1.13  1.21  53.39 -0.9 -0.26
730 | 2.53  -1.27  0.7 -0.9  64.34 -0.42
731 | -4  -0.4  -0.58 -0.26 -0.42  51.7
```

```
732 |
733 | C_Hill = tensor (size: 3 3 3 3)
734 | rank: 4
735 |
736 | tensor in Voigt matrix representation
```

737	205.28	57.36	65.54	-0.17	2.54	-4
738	57.36	171.45	60.74	1.03	-1.05	-0.33
739	65.54	60.74	194.92	1.04	0.91	-0.64
740	-0.17	1.03	1.04	57.36	-0.84	-0.31
741	2.54	-1.05	0.91	-0.84	67.72	-0.45
742	-4	-0.33	-0.64	-0.31	-0.45	55.49

743 One notices, that there is a difference between the average tensors calculated directly  
744 from the EBSD data and the average tensors calculated from the estimated ODF. These  
745 differences result from the smoothing effect of the kernel density estimation (*cf* Boogaart,  
746 2001). The magnitude of the difference depends on the actual choice of the kernel. It is  
747 smaller for sharper kernels, or more precisely for kernels with leading Fourier coefficients  
748 close to 1. An example for a family of well suited kernels can be found in Hielscher (2010).

## 749 Conclusions

750 An extensive set of functions have been developed and validated for the calculation of  
751 anisotropic crystal physical properties using Cartesian tensors for the MTEX open source  
752 MatLab toolbox. The functions can be applied to tensors of single or polycrystalline  
753 materials. The implementation of the average tensor of polycrystalline and multi-phase  
754 aggregates using the Voigt, Reuss and Hill methods have been made using three routes;  
755 a) the weighted summation for individual orientation data (e.g. EBSD), b) the weighted  
756 integral of the ODF, and c) using the Fourier coefficients of the ODF. Special attention  
757 has been paid to the crystallographic reference frame used for orientation data (e.g. Euler  
758 angles) and Cartesian tensors, as these reference frames are often different in low sym-  
759 metry crystals and dependent on the provenance of the orientation and tensor data. The  
760 ensemble of MTEX functions can be used to construct project specific MatLab M-files,  
761 to process orientation data of any type in a coherent work-flow from the texture analysis  
762 to the anisotropic physical properties. A wide range of graphical tools provides publi-  
763 cation quality output in a number of formats. The construction of M-files for specific  
764 problems provides a problem-solving method for teaching elementary to advanced tex-  
765 ture analysis and anisotropic physical properties. The open source nature of this project  
766 (<http://mtex.googlecode.com>) allows researchers to access all the details of their cal-  
767 culations, check intermediate results and further the project by adding new functions on  
768 Linux, Mac OSX or Windows platforms.

## 769 Acknowledgments

770 The authors gratefully acknowledge that this contribution results from scientific coop-  
771 eration on the research project “Texture and Physical Properties of Rocks”, which has  
772 been funded by the French-German program EGIDE-PROCOPE. This bilateral program  
773 is sponsored by the German Academic Exchange Service (DAAD) with financial funds  
774 from the federal ministry of education and research (BMBF) and the French ministry of  
775 foreign affairs.

776 We would like to dedicate this work to the late Martin Casey (Leeds) who had written  
777 his own highly efficient FORTRAN code to perform pole figure inversion for low symmetry  
778 minerals using the spherical harmonics approach of Bunge (Casey,1981). The program  
779 source code was freely distributed by Martin to all interested scientists since about 1979,  
780 well before today's open source movement. Martin requested in July 2007 that DM made  
781 his own FORTRAN code open source, in response to that request we have extended MTEX  
782 to include physical properties in MatLab, a programming language more accessible to young  
783 scientists and current teaching practices.

## 784 A The Fourier coefficients of the rotated Tensor

785 In this section we are concerned with the Fourier coefficients of tensors as they are required  
786 in equation (8). Previous work on this problem can be found in Jones (1985). However,  
787 in this section we present explicit formulas for the Fourier coefficients  $\hat{T}_{m_1, \dots, m_r}(J, L, K)$  in  
788 terms of the tensor coefficients  $T_{m_1, \dots, m_r}(g)$ . In particular, we show that the order of the  
789 Fourier expansion is bounded by the rank of the tensor.

Let us first consider the case of a rank one tensor  $T_m$ . Given an orientation  $g \in \text{SO}(3)$   
the rotated tensor may expressed as

$$T_m(g) = T_n R_{mn}(g)$$

where  $R_{ij}(g)$  is the rotation matrix corresponding to the orientation  $g$ . Since the entries of  
the rotation matrix  $R(g)$  are related with the generalized spherical harmonics  $D_{\ell k}^1(g)$  by

$$R_{mn}(g) = D_{\ell k}^1 U_{m\ell} \overline{U_{nk}}, \quad U = \begin{pmatrix} \frac{1}{\sqrt{2}}i & 0 & -\frac{1}{\sqrt{2}}i \\ -\frac{1}{\sqrt{2}}i & 0 & \frac{1}{\sqrt{2}}i \\ 0 & i & 0 \end{pmatrix},$$

we obtain

$$T_m(g) = T_n D_{\ell k}^1 U_{m\ell} \overline{U_{nk}}.$$

Hence, the Fourier coefficients  $\hat{T}_m(1, \ell, k)$  of  $T_m(g)$  are given by

$$\hat{T}_m(1, \ell, k) = T_n U_{m\ell} \overline{U_{nk}}.$$

Next we switch to the case of a rank two tensor  $T_{m_1 m_2}(g)$ . In this case we obtain

$$\begin{aligned} T_{m_1 m_2}(g) &= T_{n_1 n_2} R_{m_1 n_2}(g) R_{m_2 n_2}(g) \\ &= T_{n_1 n_2} D_{\ell_1 k_1}^1(g) U_{m_1 \ell_1} \overline{U_{n_1 k_1}} D_{\ell_2 k_2}^1(g) U_{m_2 \ell_2} \overline{U_{n_2 k_2}}. \end{aligned}$$

With the Clebsch Gordan coefficients  $\langle j_1 m_1 j_2 m_2 | JM \rangle$  (cf. Varshalovich, D. A.; Moskalev, A. N.; Khersonskii, V. K. (1988). Quantum Theory of Angular Momentum. World Scientific Publishing Co..) we have

$$D_{\ell_1 k_1}^{j_1}(g) D_{\ell_2 k_2}^{j_2}(g) = \sum_{J=0}^{j_1+j_2} \langle j_1 \ell_1 j_2 \ell_2 | JL \rangle \langle j_1 k_1 j_2 k_2 | JK \rangle D_{LK}^J(g), \quad (9)$$

and, hence,

$$T_{m_1 m_2}(g) = \sum_{J=0}^2 T_{n_1 n_2} U_{m_1 \ell_1} \overline{U_{n_1 k_1}} U_{m_2 \ell_2} \overline{U_{n_2 k_2}} \langle 1 \ell_1 1 \ell_2 | J L \rangle \langle 1 k_1 1 k_2 | J K \rangle D_{LK}^J(g).$$

Finally, we obtain for the Fourier coefficients of  $T_{mm'}$ ,

$$\widehat{T}_{m_1 m_2}(J, L, K) = T_{n_1 n_2} U_{m_1 \ell_1} \overline{U_{n_1 k_1}} U_{m_2 \ell_2} \overline{U_{n_2 k_2}} \langle 1 \ell_1 1 \ell_2 | J L \rangle \langle 1 k_1 1 k_2 | J K \rangle$$

For a third rank tensor we have

$$\begin{aligned} T_{m_1 m_2 m_3}(g) &= T_{n_1 n_2 n_3} R_{m_1 n_1}(g) R_{m_2 n_2}(g) R_{m_3 n_3}(g) \\ &= T_{n_1 n_2 n_3} D_{\ell_1 k_1}^1 U_{m_1 \ell_1} \overline{U_{n_1 k_1}} D_{\ell_2 k_2}^1 U_{m_2 \ell_2} \overline{U_{n_2 k_2}} D_{\ell_3 k_3}^1 U_{m_3 \ell_3} \overline{U_{n_3 k_3}}. \end{aligned}$$

Using (9) we obtain

$$\begin{aligned} T_{m_1 m_2 m_3}(g) &= T_{n_1 n_2 n_3} D_{\ell_1 k_1}^1 U_{m_1 \ell_1} \overline{U_{n_1 k_1}} D_{\ell_2 k_2}^1 U_{m_2 \ell_2} \overline{U_{n_2 k_2}} D_{\ell_3 k_3}^1 U_{m_3 \ell_3} \overline{U_{n_3 k_3}} \\ &= \sum_{J_1=0}^2 T_{n_1 n_2 n_3} U_{m_1 \ell_1} \overline{U_{n_1 k_1}} U_{m_2 \ell_2} \overline{U_{n_2 k_2}} U_{m_3 \ell_3} \overline{U_{n_3 k_3}} \\ &\quad \langle 1 \ell_1 1 \ell_2 | J_1 L_1 \rangle \langle 1 k_1 1 k_2 | J_1 K_1 \rangle D_{L_1 K_1}^{J_1}(g) D_{\ell_3 k_3}^1 \\ &= \sum_{J_1=0}^2 \sum_{J_2=0}^{J_1+1} T_{n_1 n_2 n_3} U_{m_1 \ell_1} \overline{U_{n_1 k_1}} U_{m_2 \ell_2} \overline{U_{n_2 k_2}} U_{m_3 \ell_3} \overline{U_{n_3 k_3}} \\ &\quad \langle 1 \ell_1 1 \ell_2 | J_1 L_1 \rangle \langle 1 k_1 1 k_2 | J_1 K_1 \rangle \\ &\quad \langle J_1 L_1 1 \ell_3 | J_2 L_2 \rangle \langle J_1 K_1 1 k_3 | J_2 K_2 \rangle D_{L_2 K_2}^{J_2}(g). \end{aligned}$$

Hence, the coefficients of  $T_{m_1 m_2 m_3}$  are given by

$$\begin{aligned} \widehat{T}_{m_1 m_2 m_3}(J_2, L_2, K_2) &= \sum_{J_1=J_2-1}^2 T_{n_1 n_2 n_3} U_{m_1 \ell_1} \overline{U_{n_1 k_1}} U_{m_2 \ell_2} \overline{U_{n_2 k_2}} U_{m_3 \ell_3} \overline{U_{n_3 k_3}} \\ &\quad \langle 1 \ell_1 1 \ell_2 | J_1 L_1 \rangle \langle 1 k_1 1 k_2 | J_1 K_1 \rangle \\ &\quad \langle J_1 L_1 1 \ell_3 | J_2 L_2 \rangle \langle J_1 K_1 1 k_3 | J_2 K_2 \rangle. \end{aligned}$$

790

Finally, we consider the case of a fourth rank tensor  $T_{m_1, m_2, m_3, m_4}$ . Here we have

$$\begin{aligned}
T_{m_1, m_2, m_3, m_4} &= T_{n_1, n_2, n_3, n_4} D_{m_1, n_1}^1 D_{m_2, n_2}^1 D_{m_3, n_3}^1 D_{m_4, n_4}^1 \\
&= T_{n_1, n_2, n_3, n_4} \sum_{J_1=0}^2 \sum_{J_2=0}^2 \langle 1m_1 1m_2 | J_1 M_1 \rangle \langle 1n_1 1n_2 | J_1 N_1 \rangle D_{M_1, N_1}^{J_1} \\
&\quad \langle 1m_3 1m_4 | J_2 M_2 \rangle \langle 1n_3 1n_4 | J_2 N_2 \rangle D_{M_2, N_2}^{J_2} \\
&= T_{n_1, n_2, n_3, n_4} \sum_{J_0=0}^4 \sum_{J_1=0}^2 \sum_{J_2=0}^2 \langle 1m_1 1m_2 | J_1 M_1 \rangle \langle 1n_1 1n_2 | J_1 N_1 \rangle \\
&\quad \langle 1m_3 1m_4 | J_2 M_2 \rangle \langle 1n_3 1n_4 | J_2 N_2 \rangle \\
&\quad \langle J_1 M_1 J_2 M_2 | J_0 M_0 \rangle \langle J_1 N_1 J_2 N_2 | J_0 N_0 \rangle D_{M_0, N_0}^{J_0},
\end{aligned}$$

and, hence,

$$\begin{aligned}
\hat{T}_{m_1, m_2, m_3, m_4}(J_0, M_0, N_0) &= \sum_{J_1=0}^2 \sum_{J_2=0}^2 \langle 1m_1 1m_2 | J_1 M_1 \rangle \langle 1n_1 1n_2 | J_1 N_1 \rangle \\
&\quad \langle 1m_3 1m_4 | J_2 M_2 \rangle \langle 1n_3 1n_4 | J_2 N_2 \rangle \\
&\quad \langle J_1 M_1 J_2 M_2 | J_0 M_0 \rangle \langle J_1 N_1 J_2 N_2 | J_0 N_0 \rangle.
\end{aligned}$$

## References

791

- 792 [1] Aleksandrov, K.S., Alchikov, U.V., Belikov, B.P., Zaslavskii, B.I. & Krupnyi, A.I.:  
793 1974, 'Velocities of elastic waves in minerals at atmospheric pressure and increasing  
794 precision of elastic constants by means of EVM (in Russian)', Izv. Acad. Sci. USSR,  
795 Geol. Ser. 10, 15-24.
- 796 [2] Bachmann, F., Hielscher, H., Jupp, P. E., Pantleon, W., Schaeben, H. & Wegert, E.:  
797 2010. Inferential statistics of electron backscatter diffraction data from within individual  
798 crystalline grains. J. Appl. Cryst. 43, 1338-1355
- 799 [3] Bass J.D., 1995. Elastic properties of minerals, melts, and glasses, in: Handbook of  
800 Physical Constants, edited by T.J. Ahrens, American Geophysical Union special publi-  
801 cation, pp. 45-63.
- 802 [4] Bezacier, L., Reynard, B., Bass, J.D., Wang, J., & Mainprice, D., 2010. Elasticity of  
803 glaucophane and seismic properties of high-pressure low-temperature oceanic rocks in  
804 subduction zones. Tectonophysics, 494, 201-210.
- 805 [5] Bunge, H.-J., 1968, Über die elastischen konstanten kubischer materialien mit beliebiger  
806 textur. Kristall und Technik 3, 431-438.

- 807 [6] Casey, M., 1981. Numerical analysis of x-ray texture data: An implementation in  
808 FORTRAN allowing triclinic or axial specimen symmetry and most crystal symmetries.  
809 Tectonophysics, 78, 51-64.
- 810 [7] Christoffel, E.B., 1877. Über die Fortpflanzung van Stößen durch elastische feste  
811 Körper. Annali di Matematica pura ed applicata, Serie II 8, 193-243.
- 812 [8] Fei Y., 1995. Thermal expansion, in Minerals physics and crystallography: a handbook  
813 of physical constants, edited by T.J. Ahrens, pp. 29-44, American Geophysical Union,  
814 Washington D.C.
- 815 [9] Ganster, J., and Geiss, D. (1985) Polycrystalline simple average of mechanical proper-  
816 ties in the general (triclinic) case. Phys. stat. sol. (b) , 132, 395-407.
- 817 [10] R. Hielscher, 2010. Kernel density estimation on the rotation group, Preprint, Fakultät  
818 für Mathematik, TU Chemnitz.
- 819 [11] R. Hielscher, H. Schaeben, H. Siemes, 2010. Orientation distribution within a single  
820 hematite crystal. Math. Geosci., 42, 359-375.
- 821 [12] Hielscher,R., & Schaeben,H., 2008, A novel pole figure inversion method: spec-  
822 ification of the MTEX algorithm. Journal of Applied Crystallography, 41 ,1024-  
823 1037.doi:10.1107/S0021889808030112
- 824 [13] Hill, R., 1952. The elastic behaviour of a crystalline aggregate, Proc. Phys. Soc. Lon-  
825 don Sect. A 65 , 349-354.
- 826 [14] Hofer, M. & Schilling, F.R., 2002. Heat transfer in quartz, orthoclase, and sanidine,  
827 Phys.Chem. Minerals, 29, 571-584.
- 828 [15] Humbert, M. & Diz, J ., 1991. Some practical features for calculating the polycrys-  
829 talline elastic properties from texture, J. Appl. Cryst. 24 , 978-981.
- 830 [16] Isaak D.G., 2001. Elastic properties of minerals and planetary objects. In Handbook of  
831 Elastic Properties of Solids, Liquids, and Gases, edited by Levy, Bass and Stern Volume  
832 III: Elastic Properties of Solids: Biological and Organic Materials, Earth and Marine  
833 Sciences, pp.325-376. Academic Press
- 834 [17] Jones, M.N., 1985. Spherical harmonics and tensors for classical field theory. Research  
835 Studies Press, Letchworth, England. pp230.
- 836 [18] Kneer, G., 1965. Über die berechnung der elastizitätsmoduln vielkristalliner aggregate  
837 mit textur, Phys. Stat. Sol., 9 , 825-838.
- 838 [19] Mainprice, D., 1990. An efficient FORTRAN program to calculate seismic anisotropy  
839 from the lattice preferred orientation of minerals. Computers & Geosciences,16,385-393.



- 840 [20] Mainprice, D. & Humbert, M., 1994. Methods of calculating petrophysical properties  
841 from lattice preferred orientation data. *Surveys in Geophysics* 15, 575-592.
- 842 [21] Mainprice, D., 2007. Seismic anisotropy of the deep Earth from a mineral and rock  
843 physics perspective. Schubert, G. *Treatise in Geophysics Volume 2* pp437-492. Oxford:  
844 Elsevier.
- 845 [22] Mainprice, D., Le Page, Y., Rodgers, J. & Jouanna, P., 2008. *Ab initio* elastic prop-  
846 erties of talc from 0 to 12 GPa: interpretation of seismic velocities at mantle pressures  
847 and prediction of auxetic behaviour at low pressure. *Earth and Planetary Science Letters*  
848 274, 327-338. doi:10.1016/j.epsl.2008.07.047
- 849 [23] Morris, P.R., 2006. Polycrystalline elastic constants for triclinic crystal and physical  
850 symmetry, *J. Applied Crystal.*, 39,502-508.
- 851 [24] Nye, J. F., 1985. *Physical Properties of Crystals: Their Representation by Tensors*  
852 *and Matrices*, 2nd ed., Oxford Univ. Press, England.
- 853 [25] Reuss, A., 1929. Berechnung der Fließrenze von Mischkristallen auf Grund der Plas-  
854 tizitätsbedingung für Einkristalle, *Z. Angew. Math. Mech.* 9, 49-58.
- 855 [26] Sirotin, Yu.I. & Shakolskaya, M.P., 1982. *Fundamentals of Crystal Physics*. Mir,  
856 Moscow. pp 654.
- 857 [27] van den Boogaart, K. G. , 2001. *Statistics for individual crystallographic orientation*  
858 *measurements*. Phd Thesis, Shaker.
- 859 [28] Voigt,W., 1887. Theoretische studien über die elastizitätsverhältnisse. *Abh. Gött.*  
860 *Akad. Wiss.*, 48-55.
- 861 [29] Voigt,W., 1928. *Lehrbuch der Kristallphysik*, Teubner-Verlag,Leipzig.
- 862 [30] Varshalovich, D. A.; Moskalev, A. N.; Khersonskii, V. K. (1988). *Quantum Theory of*  
863 *Angular Momentum*. World Scientific Publishing Co.